Single- and double-charge-exchange cross sections for $Ar^{q+}+H_2$ ($q=6$, 7, 8, 9, and 11) collisions from 6 eV to 11 keV

Scott Kravis,[1,*] Hiroki Saitoh,[2] Kazuhiko Okuno,[2] Kouichi Soejima,[2] Mineo Kimura,[3] Isao Shimamura,[1] Yohko Awaya,[1] Yozaburo Kaneko,[2] Masaki Oura,[1] and Noriyuki Shimakura[4]

[1]*The Institute of Physical and Chemical Research (RIKEN), Hirosawa 2-1, Wako-shi, Saitama, 351-01, Japan*

[2]*Department of Physics, Tokyo Metropolitan University, Minami-Ohsawa 1-1, Hachioji-shi, Tokyo 192-03, Japan*

[3]*Argonne National Laboratory, Argonne, Illinois 60439*

[4]*Faculty of Science, Niigata University, Niigata-shi, 950-21, Japan*

(Received 19 September 1994; revised manuscript received 25 April 1995)

The cross sections for single-electron capture, including transfer ionization, and for double-electron capture, have been measured for $Ar^{q+}+H_2$ for $q=6$, 7, 8, 9, and 11 with projectile energies from q eV to q keV. Theoretically, the cross sections for Ar^{6+} and Ar^{8+} impact were calculated using a molecular-orbital expansion method in the energy region from 240 eV to 80 keV, and are in good agreement with experiment. The single-electron-capture cross sections were found to be more than one order of magnitude larger than those for double capture in both experiment and theory. The single-electron-capture cross sections were also compared to the Langevin cross section, a scaling law developed by Müller and Salzborn [Phys. Lett. **62A**, 391 (1977)], and the absorbing sphere model.

PACS number(s): 34.70.+e

I. INTRODUCTION

Accurate determination of cross sections for electron capture in ion-atom and ion-molecule collisions is an essential ingredient for understanding various applications in applied sciences and technologies such as ionospheric research, the study of synthesis of molecules in interstellar space, astrophysical plasmas [1] and laboratory plasmas for fusion research [2]. Many measurements with collision energies above 5 keV exist for multicharged ions, but data below 5 keV are scarce and low-energy data below 100 eV were almost nonexistent until recently due to the difficulty of handling very-low-energy, multiply charged ion beams. With the utilization of the octupole ion-beam guide (OPIG) [3] ion-beam transport has become possible down to q eV energies. This paper describes measurements, using the OPIG technique, of single- and double-electron capture in $Ar^{q+}+H_2$ ($q=6$, 7, 8, 9, and 11) collisions with projectile energies from 6 eV to 11 keV. Our single-electron-capture cross sections are the sum of the two following reactions:

$$\begin{aligned} &Ar^{q+}+H_2 \Longrightarrow Ar^{(q-1)+}+H_2^{+} \text{ (or } 2H^{+}+e\text{)}, \\ &Ar^{q+}+H_2 \Longrightarrow [Ar^{(q-2)+}]^{**}+2H^{+} \Longrightarrow Ar^{(q-1)+}+e+2H^{+}, \end{aligned} \tag{1}$$

where the first reaction is direct single-electron capture. The second reaction corresponds to the transfer ionization process where two electrons are transferred into a doubly excited state of the ion (denoted by **) and it decays via an Auger-type process where one electron is emitted and the other one subsequently makes a transition(s) to an orbital with lower energy, leaving the ion in the ground state. Our double-electron-capture cross sections correspond to the reaction

$$Ar^{q+}+H_2 \Longrightarrow Ar^{(q-2)+}+2H^{+}. \tag{2}$$

Theoretically, very little attention had been directed towards the H_2 target until recently, mainly because of the difficulty in treating the multicenter nature of the molecular field accurately [4]. However, renewed interest was stimulated primarily by more precise and detailed experimental information on H_2. This, coupled with advanced development of sophisticated theoretical treatments, began to reveal interesting but complex physics and has shed light on collision systems involving H_2 within a few years [4,5]. Therefore it became feasible to calculate some of the measured cross sections in a more sophisticated treatment than previously possible, using the molecular-orbital expansion method [4].

Charge-changing-collision cross sections from thermal energies to hundreds of eV are of crucial importance for the analysis of some experiments using various types of ion traps that operate in an ultrahigh-vacuum environment, such as Penning ion traps and electron-beam ion traps (EBIT's) [6] These devices can store multiply charged ions for long periods of time, during which charge-changing collisions with the neutral background gas can modify the charge-state distribution of the confined ions. The reader is reminded that H_2 is usually the dominant residual gas in an ultrahigh-vacuum environment. Detailed calculations of the charge-transfer cross section by techniques such as the molecular-orbital expansion method require complete information of the three-dimensional surface of the adiabatic interaction potentials, which it is a formidable task to calculate even by

*Present address: J. R. Macdonald Laboratory, Kansas State University, Manhattan, KS 66506.

supercomputers. Accordingly, some types of simplifications are employed to reduce numerical complexities, based on the ratio of the collision time to the vibrational period of the molecular target. This simplification is known to be accurate down to a few tens of eV/amu in collision energy. Therefore, below the energy region where the present theory is less applicable, we apply simple models such as the Langevin (orbiting) model [7] and the absorbing sphere model [8] to examine the energy dependence and magnitude of the cross sections measured here. We also compare the high-energy end of our results with a scaling formula proposed by Müller and Salzborn [9]. Previous experimental data [10–13] from other groups are also presented.

II. EXPERIMENTAL SETUP

The technique used was reported elsewhere in more detail [3,14,15], so only a brief description of the experimental setup will be given here. Figure 1 shows a schematic diagram of the experimental setup. Ions were extracted from a mini-EBIS (electron-beam ion source) in the continuous mode and then the desired charge state was selected by an analyzing magnet (MS1). Before the OPIG the ion beam is collimated by 0.5-mm-diameter slits, and the OPIG entrance aperture is 1 mm in diameter. The beam is decelerated by a retarding voltage at the entrance of the OPIG and guided along the axis of the collision cell by the rf supplied to the beam guide. The inscribed circle of the eight poles of the OPIG is 4 mm in diameter. Upon exciting the collision region the beam was reaccelerated, charge-state analyzed (MS2), and detected by a secondary-electron multiplier. The ions were counted for a preset time and then the data from the counter were transferred to a personal computer. The rate of the parent ion-beam flux was kept below 10 000 sec^{-1} to prevent counting loss due to the pileup of the signal pulses. The pressure in the collision cell was monitored by a calibrated pressure gauge. The effective interaction length inside the OPIG was estimated to be 9.0 cm by careful consideration of pressure gradients, conductance measurements, and comparison of measured resonant charge-transfer data with previously measured data. The target pressures used were below 1.5×10^{-5} Torr, assuring single-collision conditions. Also measurements were made as a function of target pressure to confirm single-collision conditions. After determining the interaction length and target H_2 density, the experimental cross sections were found by first measuring the primary Ar^{q+} ion-beam intensity without the H_2 target and then measuring the charge-changed product ions with the H_2 target. In this collision system ($Ar^{q+}+H_2$) where the projectile is much heavier than the target, off-axis deflections of projectiles caused by collisions are small. Therefore transport of the product ions through the OPIG is nearly 100%. The use of the OPIG made these low-energy measurements possible. The overall uncertainty in the measured cross section is estimated to be ±20%. The main contribution to the uncertainty of the measurements is from determination of the target density and interaction length. The zero point of and uncertainty in projectile energy were estimated by measuring the ion transmission through the OPIG as a function of the retarding voltage. The ion energy uncertainty was found to be $\pm0.4q$ eV.

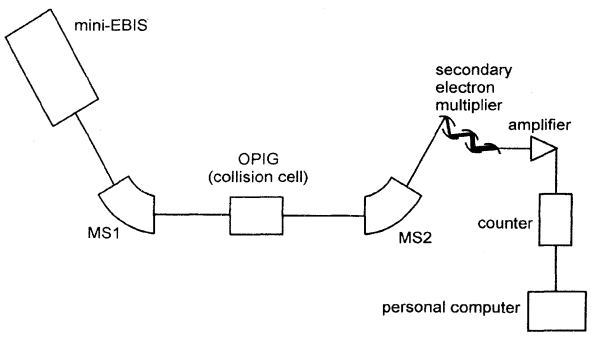

FIG. 1. Geometry of the experimental setup.

The exact states and quantities of electronically excited ions from the EBIS have not been measured, but due to the relatively long time the ions spend inside the EBIS (>10 μsec) large quantities of excited ions are not expected.

III. THEORY

A. Molecular-orbital expansion method

Details of our theoretical description of the molecular representation have been given previously [4]. However, we will provide a short summary of this method.

A semiclassical molecular-orbital expansion method was used to study the collision dynamics, which is believed to be valid in the collision energy region above a few 10 eV/amu. Molecular states of the system $(ArH_2)^{q+}$ were obtained by the configuration-interaction (CI) method with Slater-type orbitals (STO's). In this CI calculation, the two H_2 electrons were treated explicitly, while the effect of the more tightly bound electrons of the Ar ions was represented by Gaussian-type pseudopotentials [16]. These pseudopotentials were determined so as to reproduce the energy levels of $Ar^{(q-1)+}$. Thus the net interactions of all the electrons in the ground-state $Ar^{8+}(1s^22s^22p^6)$ $[Ar^{6+}(1s^22s^22p^63s^2)]$ with the other electrons were represented by pseudopotentials for Ar^{8+} (Ar^{6+}) impact. The H_2 molecules were approximated by an atom having an average first- and second-ionization potential of 15.8–16.1 and 31.7 eV, respectively. The average here means that over the vibrational wave function squared. This approximate treatment has been proven to be reasonably accurate in the energy region where vibrational excitation processes are not expected to play an important role in the dynamics [4]. After careful examination of the convergence in the energy levels, 24–28 STO's were used to represent the Ar ions and six STO's for the H_2 molecule as a basis set for the CI calculation. The asymptotic energy levels in the separated-atom limit were in good agreement (within 0.2%) with spectroscopic data [17].

Several sets of close-coupling calculations using straight-line trajectories for the heavy-particle motion, including different molecular states were carried out to assess the convergence and to identify dominant collision mechanisms or reaction paths. A typical set included (i) the initial channel $Ar^{q+}+H_2$, (ii) representative single-electron-transfer channels $Ar^{(q-1)+}(n=3,4)+H_2^+$, and (iii) some double-electron-transfer channels

$$Ar^{(q-2)+}+(n=3,n'=3,4,5)+2H^+ .$$

In some test calculations double capture into autoionizing states $Ar^{(q-2)+}(n=4,n'=4)$ was explicitly taken into account, and its cross section dominated over the cross section for double capture into true bound states. However, these autoionizing states decay into $Ar^{(q-1)+}(n=3)+e^-$ and contribute to the transfer ionization cross section, which is included in the single-electron-capture cross section as defined earlier in the second reaction of Eq. (1). Since this contribution is small compared with the total single-electron-capture cross section, we ignored double capture into autoionizing states in our production run.

B. Scaling analysis

As discussed earlier, in order to check the energy dependence and magnitude of the cross sections, particularly in the low-energy region, we apply the following scaling analyses. This procedure also provides information of the applicability of each scaling formula.

1. Müller and Salzborn

Müller and Salzborn developed an empirical scaling law [8] for charge-transfer cross sections from 107 data points for single-electron transfer and 77 data points for double-electron transfer, ranging in collision energy from about 10 to 100 keV for various collision systems. The scaling law is in terms of q and I, the ionization potential of the target in eV,

$$\sigma_{MS}=Aq^{\alpha}I^{\beta} . \tag{3}$$

A, α, and β are fitting parameters and equal to $(1.43\pm0.76)\times10^{-12}$ cm^2, 1.17 ± 0.09, and -2.76 ± 0.19, respectively, for single-electron transfer and $(1.08\pm0.95)\times10^{-12}$ cm^2, 0.71 ± 0.14, and -2.80 ± 0.32 for double-electron transfer. In the energy range of the collisions from which the scaling law was derived it was believed that the capture cross sections would have little energy dependence (which is reflected in the scaling law itself). Therefore it would be most applicable only to the high-energy end of the collisions in the present data.

2. Langevin cross section

In the limit of low collision energies, the interaction potential of the longest range, namely, the attractive polarization potential $V_p=-\alpha_D q^2/2R^4$, is the most significant in ion-atom collisions. α_D is the dipole polarizability of the target and R is the distance between the target and projectile. The projectile follows a spiral orbit in this potential, falling into a region of small R, whenever the impact parameter b is less than the critical value

$$b_0=\left[\frac{4q^2\alpha_D}{\mu v_r^2}\right]^{1/4} , \tag{4}$$

where v_r is the relative velocity of the collision and μ is the reduced mass of the collision system. Therefore, if there is a crossing between diabatic potential-energy curves at an R_x smaller than b_0, a projectile with $b<b_0$ has a high probability of undergoing a charge-transfer process. If this probability is approximated by 1, an upper limit of the low-energy charge-transfer cross section is

$$\sigma_L=\pi b_0^2 , \tag{5}$$

and is called the Langevin cross section [7].

Two kinds of limitations of this model warrant remarks here. Since this model assumes a charge-transfer probability of zero for $R>b_0$, σ_L may not be an upper limit if there is an R_x larger than b_0. Furthermore, if the target is not an atom but a *molecule* with a dipole moment D and a quadrupole moment Q, there exist interaction potentials of even longer range than V_p, namely, the dipole potential $V_D\propto qD/R^2$ and the quadrupole potential $V_Q\propto qQ/R^3$, both of which depend on the molecular orientation. Hence these potentials must be more important than V_p in the low-energy limit. However, D is zero and Q is small for the molecule of our interest, H_2. Also the large q values in the present experiment put more importance on V_p, which behaves as q^2, unlike the behavior of V_D and V_Q, which are proportional to q. Thus V_Q and V_D play a significant role only at extremely low collision energies [18], which have not been reached in this work. The Langevin cross section has been shown to be applicable at near thermal energies for both singly and multiply charged ions [7,12] when the critical impact parameter b_0 is larger than the charge-capture crossing radius. At much higher energies b_0 becomes small and orbiting is unlikely to occur.

3. Absorbing sphere model

The third model used was developed by Olson and Salop and is termed the absorbing sphere model [9]. This model is based on the Landau-Zener (LZ) theory. When there is a large number of curve crossings between a single initial state and a band of final states inside some critical distance R_c, the charge-transfer probability inside this R_c can be assumed to be unity. Then the charge-transfer cross section can be approximated as

$$\sigma_{OS}=\pi R_c^2 . \tag{6}$$

Combining information from a compilation of a large volume of adiabatic potentials and couplings and additional calculations for simpler one-electron diatomic molecular systems, Olson and Salop derived an equation (in atomic units) that determines R_c semiempirically, namely,

$$R_c^2 e^{-2.648\alpha R_c/q^{1/2}}=2.864\times10^{-4}q(q-1)v_0/f \tag{7}$$

TABLE I. Present experimental cross sections for single- and double-charge capture for $Ar^{q+}+H_2$ as a function of the center-of-mass energy over q. The cross sections are in units of 10^{-15} cm^2 and $E_{c.m.}/q$ is in eV.

	Single capture					Double capture				
$E_{c.m.}/q$	$q=6$	$q=7$	$q=8$	$q=9$	$q=11$	$q=6$	$q=7$	$q=8$	$q=9$	$q=11$
0.02	24.8		18.8	33.6	37.8	2.14		3.46	1.77	3.70
0.05	23.5	26.8	17.9	31.6	34.5	1.52	2.14	2.88	1.53	3.03
0.07	21.2	25.1	16.0			1.25	1.77	2.51		
0.10	20.0	23.3	14.9	30.7	34.6	1.12	1.42	2.25	1.34	2.58
0.14	18.5	20.7	13.3			0.97	1.16	1.85		
0.19	16.1	18.2	12.3	25.4	32.5	0.89	0.94	1.45	1.28	2.22
0.24			11.5					1.39		
0.33	15.2	16.9	10.9			0.78	0.79	1.23		
0.48	13.4	15.2	10.2	20.9	32.0	0.71	0.69	1.03	1.07	2.15
0.95	11.7	13.5	9.33	19.5	27.0	0.62	0.61	0.70	1.03	2.16
1.43			8.78					0.57		
1.90	10.5	11.6	8.49	17.6	25.8	0.61	0.55	0.46	0.98	1.95
2.38			8.58					0.46		
3.33	10.0	11.4	8.55			0.59	0.55	0.41		
4.76	10.3	11.4	8.70	17.3	22.9	0.67	0.62	0.50	0.87	2.02
9.52	8.26	9.90	7.57	15.8	21.6	0.53	0.52	0.34	0.66	1.89
15.24	7.67					0.61				
19.05	7.21	10.3	8.22	13.4	22.3	0.62	0.50	0.32	0.48	2.30
33.33	7.36	9.75	7.14			0.63	0.47	0.27		
47.61	7.05	9.09	7.54	12.1	20.5	0.52	0.34	0.25	0.26	1.77
71.42		8.93					0.27			

with $\alpha=[I/13.6\ (\text{eV})]^{1/2}$ where v_0 is the incident velocity of the projectile and f is the Franck-Condon factor for specific transitions between vibrational levels. A Franck-Condon factor of 1 was used in our calculation. The absorbing sphere model is most applicable for high q where there are a large number of Ar^{q-1} excited levels available for the reaction and when $v_0 \leq 1\times10^8$ cm/sec.

IV. RESULTS

The results of our experiment are shown in Figs. 2(a)–2(e) along with the molecular-orbital expansion calculations, Langevin theory, Müller-Salzborn scaling law, and Olson and Salop's absorbing sphere model. Our experimental and theoretical results are also tabulated in Tables I and II, respectively. Also presented in the figures are previous data from Can *et al.* [10], Hanaki *et al.* [11], Kravis *et al.* [12], and Vancura *et al.* [13]. For Ar^{6+} the molecular-orbital expansion calculation lies about 50% below the experimental values for both single and double capture. In the Ar^{8+} case the calculation is in better agreement with experiment for both single and double capture. The general trends of the experimental results and molecular-orbital expansion calculation are in good agreement with each other.

A general feature for all the data is that the single-capture cross sections are more than an order of magnitude larger than the double-capture cross section, and calculations by the molecular-orbital expansion method confirm this for $Ar^{6,8+}$. One can also see that the character of the cross-section energy dependence changes between Ar^{8+} and Ar^{9+}. For Ar charge states with $q \leq 8$, both the single- and double-electron-capture cross sections have small slopes (increasing from high to low energies) at the high-energy end of the data but have an increase in slope near the low-energy end of the data. For Ar^{9+} a different energy dependence is seen, specifically, a larger slope at the higher energies and a smaller slope at the low energies. The energy dependence for double-electron capture by Ar^{11+} is nearly flat until the lowest energies, where it increases slightly. For single-electron capture by Ar^{11+} the energy dependence has a constant slow increase in cross section from high to low energy.

TABLE II. Present theoretical cross sections for single- and double-charge capture for $Ar^{q+}+H_2$ as functions of the center-of-mass energy. The cross sections are in units of 10^{-15} cm^2 and $E_{c.m.}$ is in eV.

	Single		Double	
$E_{c.m.}$	$q=6$	$q=8$	$q=6$	$q=8$
11.4	6.57	7.03	0.438	0.531
15.2	6.33	6.98	0.441	0.511
19	6.03	6.92	0.436	0.496
38	5.52	6.78	0.411	0.451
76	5.12	6.56	0.386	0.436
152	4.45	6.08	0.355	0.411
190	4.21	5.78	0.371	0.397
380	3.88	5.38	0.287	0.342
760	3.38	4.94	0.261	0.303
1520	3.31	4.76	0.245	0.281
1900	3.28	4.65	0.241	0.277
3800	3.21	4.58	0.242	0.280

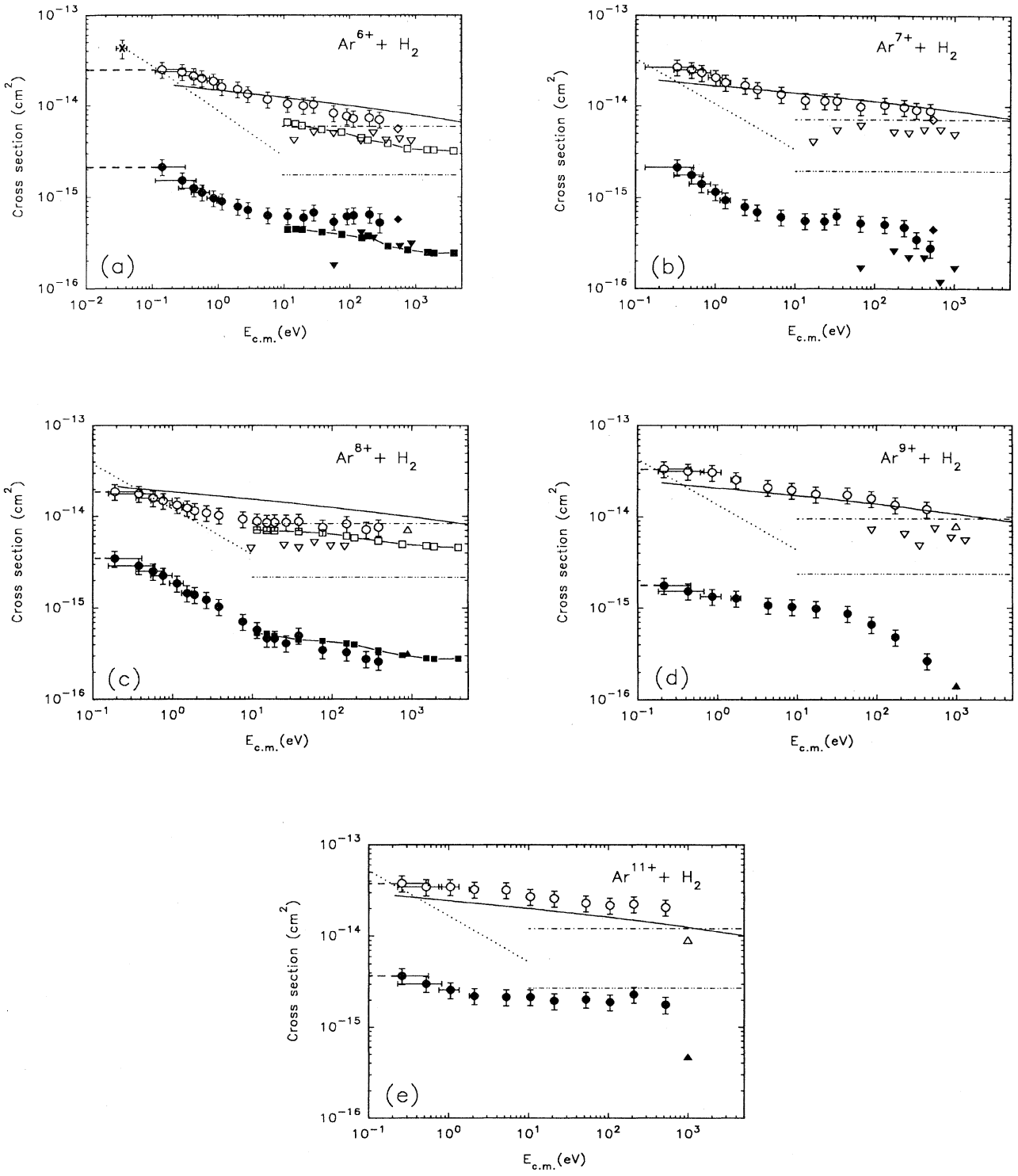

FIG. 2. Experimental and theoretical cross sections for single- and double-charge capture for $Ar^{6,7,8,9,11+}$ (a)–(e). Legend (SC=single capture, DC = double capture): ○ = present experiment SC, ● = present experiment DC, □ = MO calculation SC, ■ = MO calculation DC, ▽ = Can *et al.* [10] SC, ▼ = Can *et al.* [10] DC, ◇ = Hanaki *et al.* [11] SC, ◆ = Hanaki *et al.* [11] DC, △ = Vancura *et al.* [13], SC, ▲ = Vancura *et al.* [13] DC, * = Kravis *et al.* [12] DC+SC, –·–· Müller and Salzborn SC, –··–··–·· Müller and Salzborn DC, —— absorbing sphere SC, and · · · · Langevin SC+DC. Error bars for the present experimental data are not shown in the cases where they are smaller than the data symbol. The horizontal dashed lines to the left of some of the lowest-energy data points indicate that the error bar extends beyond the vertical axis, since the energy is plotted on a logarithmic scale.

These changes in energy dependence may be attributed to the creation of a hole(s) in the L shell of Ar^{q+}, for $q \geq 9$. The single- and double-electron-capture cross sections generally increase as a function of projectile charge state q, except for single-electron capture of Ar^{8+}, which seems to be low.

The data of Can *et al.* ($Ar^{6,7+}$ single and double capture, Ar^{8+} single capture) overlap with our data at the high-energy end. The present experimental results tend to be slightly larger than the data of Can *et al.* The data from Vancura *et al.* ($Ar^{8,9,11+}$ single and double capture) and Hanaki *et al.* ($Ar^{6,7+}$ single and double capture) are at slightly higher energies than our data, but if extrapolated to higher energies our data are in good agreement with their data.

Brief remarks about the scaling analysis are given here. The absorbing sphere model is in reasonable agreement with the $Ar^{6,7,9,11+}$ data from $E_{c.m.} \approx 1$ eV and above. The agreement with the Ar^{8+} data is generally not good.

Using the mean values for the fitting coefficients, the Müller-Salzborn scaling law, for single-electron transfer, is in reasonable agreement with experiment only at the higher energies for $Ar^{6,7,9,11+}$. For Ar^{8+} reasonable agreement is found down to $E_{c.m.} \approx 10$ eV, due to the fact that the Ar^{8+} cross section has little energy dependence in this energy region. For double-electron capture the agreement is poor. Since Müller and Salzborn derived the scaling law from data with projectile energies from a few keV to 100 keV, and since this law has no energy dependence, it would not be expected to represent our low-energy data.

In Langevin theory, the cross section for the orbiting-type collision is inversely proportional to the relative velocity v_r (see Sec. III B), so for high energies the Langevin cross section becomes small and underestimates the data. At the lowest energies the Langevin cross section is in good agreement with the present data. It is unclear from the experimental results what the energy dependence will be at even lower energies except for Ar^{6+} where one data point [12] exists at near-thermal energy (about $E_{lab} \approx 50$ meV), and agrees well with the Langevin cross section. The cross section was derived from a measurement of the rate coefficient $k = \sigma v$ for single- plus double-charge capture by estimating the velocity of the collision. Interpolation between the present data and the near-thermal-energy data would reveal an increasingly better agreement of the experimental results with the Langevin cross section for Ar^{6+} at lower energies.

V. CONCLUSION AND SUMMARY

The cross sections for single- and double-charge transfer have been measured for the collision system $Ar^{q+} + H_2$ ($q = 6$, 7, 8, 9, and 11) with projectile energies ranging from q eV to q keV. These very-low-energy measurements were made possible by use of an octupole ion-beam guide to prevent ion-beam losses.

Theoretical results were obtained by molecular-orbital expansion calculations, using a 24–28-molecular-state close-coupling method within a semiclassical formalism for Ar^{6+} and $Ar^{8+} + H_2$ collisions. The theoretical and experimental results are found to be in good agreement in energy-dependence and absolute value for Ar^{8+} projectiles, and to a somewhat lesser degree in absolute value for Ar^{6+}, for both single- and double-electron capture in the entire energy region calculated. The dominant single-electron-capture channels are found to be $Ar^{5,7+}(n=4)$ manifolds, followed by $Ar^{5,7+}(n=3)$ manifolds. Because the dominant reaction window for double-electron capture is at much smaller crossing radii than that for single-electron capture, double-electron capture is found to be much weaker for both the Ar^{6+} and Ar^{8+} collision systems. Perhaps the situation for adiabatic potentials for other charge states of Ar projectiles is similar to $Ar^{6,8+}$ since double-electron capture is the weaker of the two channels for all the charge states studied here. We assumed in the present calculation that all H_2 target molecules are in the ground vibrational state. In order to investigate temperature effects some limited test calculations for treating vibrationally excited H_2 molecules were carried out by including levels up to $v=3$. The cross sections were found to increase by about 20% at 10 eV when all H_2 molecules were assumed to be in the $v=3$ level.

Mean values for the Müller-Salzborn scaling-law coefficients were only adequate for reproducing the single-electron-transfer cross sections at the highest energies of the present data (q keV). For a rough estimation of the single-electron-capture cross sections over the entire energy range and charge states (except for $q=8$), the absorbing sphere model reasonably reproduced the data. The Langevin cross section fell well below all of our data for single-electron capture except at the lowest energies (q eV). For the Ar^{6+} case a single data point previously measured agrees well with the Langevin cross section, suggesting its usefulness at low energies.

The current data and their comparison with theory presented are near the limits of theory and experiment in low-energy charge-transfer collisions with multiply charged ions. The low-energy limit the theory can access is dictated by trajectory and vibrational excitation effects. Experimentally, a multiply charged ion source with a lower energy spread and new techniques in ion deceleration are necessary to push the low-energy limit. It would be interesting if accurate theoretical calculations could be compared with experiments at lower energies than treated in this paper. Lower-energy measurements may also shed light on the effects of the dipole and quadrupole moments of the potential of the target as discussed in Sec. III B. Furthermore, studies such as translational energy and/or electron-spectroscopy studies may reveal more detail as to why the cross section for single capture in the Ar^{8+} case is lower than that of Ar^{7+}.

ACKNOWLEDGMENTS

This study was partially supported by a Grant-in-Aid for Scientific Research from the Ministry of Education, Science and Culture of Japan. S. Kravis thanks the Science and Technology Agency (STA) of Japan and the

Japanese Society for the Promotion of Science (JSPS) for making his stay in Japan possible. The work of M. Kimura was supported by the U. S. Department of Energy, Office of Energy Research, Office of Health and Environment Research under Contract No. W-31-109-ENG-38. N. Shimakura was also supported by a Grant-in-Aid for Scientific Research on the Priority Area "Atomic Physics of Multicharged Ions" (Area No. 239/05238204) from the Ministry of Education, Science and Culture of Japan.

[1] T. Watanabe, I. Shimamura, M. Shimizu, and Y. Itikawa, *Molecular Processes in Space* (Plenum, New York, 1990).

[2] *Atomic Processes in Plasmas,* edited by E. S. Marmar and J. L. Terry, AIP Conf. Proc. No. 257 (AIP, New York, 1992).

[3] K. Okuno, K. Soejima, and Y. Kaneko, Nucl. Instrum. Methods Phys. Res. Sect. B **53**, 387 (1991); K. Okuno, J. Phys. Jpn. **55**, 1504 (1986).

[4] M. Kimura and N. F. Lane, Adv. At. Mol. Opt. Phys. **26**, 79 (1989).

[5] R. Shingal and C. D. Lin, Phys. Rev. A **40**, 1302 (1989).

[6] R. E. Marrs, S. R. Elliott, and D. A. Knapp, Phys. Rev. Lett. **72**, 4082 (1994); K. L. Wong, P. Beiersdorfer, M. H. Chen, R. E. Marrs, K. J. Reed, J. H. Scofield, D. A. Vogel, and R. Zasadzinski, Phys. Rev. A **48**, 2850 (1993); B. M. Penetrante, J. N. Bardsley, D. DeWitt, M. Clark, and D. Schneider, *ibid.* **43**, 4861 (1991).

[7] G. Gioumousis and D. P. Stevenson, J. Chem. Phys. **29**, 294 (1958).

[8] A. Müller and E. Salzborn, Phys. Lett. **62A**, 391 (1977).

[9] R. E. Olson and A. Salop, Phys. Rev. A **14**, 579 (1976).

[10] C. Can, T. Gray, S. L. Varghese, J. M. Hall, and L. N. Tunnel, Phys. Rev. A **31**, 72 (1985).

[11] H. Hanaki, T. Kusakabe, T. Horiuchi, I. Konomi, N. Nagai, T. Yamauchi, and M Sakisaka, Mem. Fac. Eng. Kyoto Univ. **46**, 1 (1984).

[12] S. D. Kravis, D. A. Church, B. M. Johnson, M. Meron, K. W. Jones, J. C. Levin, I. A. Sellin, Y. Azuma, N. Berrah-Mansour, and H. G. Berry, Phys. Rev. A **45**, 6379 (1992).

[13] J. Vancura, V. J. Marchetti, J. J. Perotti, and V. O. Kostroun, Phys. Rev. A **47**, 3758 (1993).

[14] K. Soejima, C. J. Latimer, K. Okuno, N. Kobayashi, and Y. Kaneko, J. Phys. B **25**, 3009 (1992).

[15] K. Okuno, K. Soejima, and Y. Kaneko, J. Phys. B **25**, L105 (1992).

[16] J. N. Bardsley, At. Phys. **4**, 299 (1974).

[17] S. Bashkin and J. R. Stoner, *Atomic Energy Levels and Grotrian Diagrams I* (North-Holland, Amsterdam, 1975).

[18] K. Takayanagi, J. Phys. Soc. Jpn. **51**, 3337 (1982).